actuators

MDPI

Article

Research on Underground Track Tracking of a New Type Shaft Boring Machine

Jinyu Sun [1,2], Xinming Chen [1,2,*], Huazhe Jiao [1,2], Qi Wang [1,2], Diantao Zheng [1,2], Yulong Han [1,2] and Ziyang Liu [1,2]

[1] College of Civil Engineering, Henan Polytechnic University, Jiaozuo 454150, China; 18339191823@163.com (J.S.); 18338091971@163.com (Z.L.)
[2] Key Laboratory of Underground Engineering and Disaster Prevention, Henan Polytechnic University, Jiaozuo 454150, China
* Correspondence: chenxinming@163.com

Abstract: A trajectory tracking control scheme is proposed in this paper to achieve unmanned underground construction of a new type of shaft boring machine. The body motion model is constructed, and the control relationship between the driving system and the body motion is deduced. MATLAB and Simulink simulate the joint of the track tracking process in the new shaft boring machine. The actual effect of the track tracking control scheme is validated by the track tracking field test of the new shaft boring machine. The results show that the new shaft boring machine can complete various complex track tracking tasks, with the maximum position error being less than 0.005 m. The running track and excavation areas of the boring machine are observed along with the track tracking field test of the new shaft boring machine, demonstrating that the track tracking control scheme makes the new shaft boring machine realize unmanned construction and verifies the co-simulation accuracy. The PID (proportional–integral–derivative control) algorithm can complete complex trajectory tracking tasks and promote the development of unmanned construction technology.

Keywords: new shaft boring machine; trajectory tracking; PID algorithm; co-simulation

check for updates

Academic Editor: Ioan Ursu

Received: 29 November 2024
Revised: 8 January 2025
Accepted: 9 January 2025
Published: 13 January 2025

Citation: Sun, J.; Chen, X.; Jiao, H.; Wang, Q.; Zheng, D.; Han, Y.; Liu, Z. Research on Underground Track Tracking of a New Type Shaft Boring Machine. *Actuators* **2025**, *14*, 27. https://doi.org/10.3390/act14010027

Copyright: © 2025 by the authors. Licensee MDPI, Basel, Switzerland. This article is an open access article distributed under the terms and conditions of the Creative Commons Attribution (CC BY) license (https://creativecommons.org/licenses/by/4.0/).

1. Introduction

The twenty-first century is the era of intelligence, where the government pays high attention to intelligent coal mine machinery [1]. The National Development and Reform Commission of China, the Energy Bureau, and eight other ministries and commissions jointly issued the "Guidance on Accelerating the Development of Intelligent Coal Mine" and "Coal Mine Key Research and Development Robot Directory", along with other documents [2]. The main goal is to achieve mining by unmanned operations by 2030. The National Mine Safety Supervision Bureau of the National Energy Administration issued the "Guidelines for Intelligent Construction of Coal Mines", which clarified the future development direction of coal mines. In other words, coal mines' high-end and intelligent transformation are promoted [3–5]. As an important engineering machinery, the shaft boring machine should respond to the needs of the times to develop new machinery and develop in the direction of unmanned operations. However, the existing shaft boring machine is bulky, the excavation size is single, and the degree of intelligence is low, which cannot meet the development needs. Therefore, it is urgent to develop new machinery. The new type of shaft boring machine can independently excavate shafts of any diameter, with broad application prospects in coal mines, water conservancy and hydropower projects,

and oil exploration. However, the low degree of intelligence and the inability to achieve unmanned construction have seriously limited machine promotion. Therefore, promoting the intelligent development of the new shaft boring machine is imperative. Intelligent key technologies include combined positioning and trajectory tracking. Trajectory tracking is the premise used to ensure the stability, accuracy, and safety of the operation process, with important research values [6,7].

The academic community has conducted in-depth research on the trajectory-tracking problem and has achieved rich results in different fields: Hua et al. [8] designed a trajectory-tracking controller for wheeled mobile robots based on Lyapunov's second method. The authors used a fuzzy controller to dynamically adjust the gain coefficient and improve the response speed of trajectory tracking. Tao et al. [9] proposed a trajectory-tracking control strategy for mining shovels by combining deep learning with trajectory tracking. This strategy does not need to be modeled for shovels and has better trajectory tracking accuracy. Guanchao et al. [10] proposed a predetermined time-adaptive trajectory-tracking control scheme, which solved the external interference problem of the four-rotor aircraft and reduced the pose error. Bo [11] explored the wheeled mobile robot's trajectory tracking control problem. The authors proposed a fixed-time trajectory tracking control scheme to achieve fast and accurate estimation of external disturbance information. Junling et al. [12] proposed a trajectory-tracking energy-saving control fusion strategy by combining model predictive control and a three-stage dynamic programming energy-saving control strategy. The authors improved the trajectory tracking accuracy by 70.47% while reducing energy consumption. Zekun et al. [13] explored a distributed drive-intelligent vehicle trajectory-tracking control algorithm based on the adaptive variable parameter MPC, improving the accuracy and stability of trajectory tracking. Yueyue et al. [14] proposed an adaptive neural network control algorithm to solve the problem of complex environments and uncertain dynamic models. The above research demonstrates that the application field of trajectory tracking is extensive. However, the research focuses on different machinery and the corresponding engineering. Targeted research should be conducted on specific mechanical and engineering requirements to achieve the trajectory tracking of new shaft boring machines.

In order to realize the unmanned construction of the new shaft boring machine, this paper combines the kinematic model of the new shaft boring machine and the special driving trajectory with the actual requirements of the project, conducts in-depth research, and proposes a trajectory-tracking control scheme. The scheme uses the PID algorithm [15] to control the movement of the body so that the new shaft boring machine can drive according to the preset route under the condition of unmanned operation and realize the unmanned excavation of the shaft.

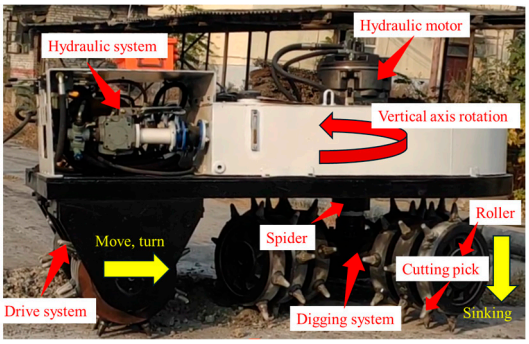
2. Trajectory-Tracking Control Mechanism

If you want to achieve the new shaft boring machine downhole trajectory tracking, you need to have a more detailed understanding of the body structure and moving trajectory. Therefore, this chapter will introduce the structure, moving trajectory, and control mechanism of the new shaft boring machine in detail. Finally, the PID algorithm is used to construct the underground control system of the new shaft boring machine.

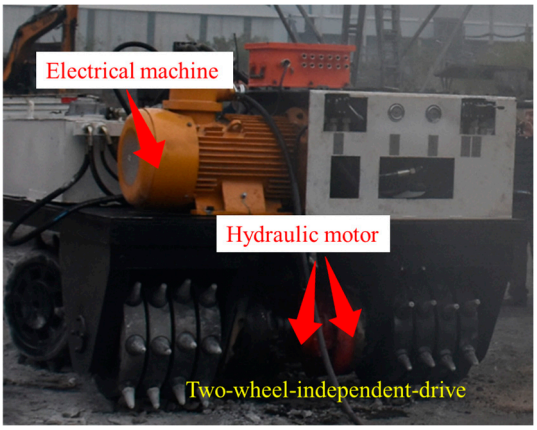
2.1. New Shaft Boring Machine Structure

The structure of the new shaft boring machine is shown in Figure 1. The boring machine mainly comprises a drive, tunneling, and hydraulic system, including a hydraulic pump, motor, drum, pick, hydraulic motor, cross shaft, and other hardware [16–18]. The hydraulic system comprises a DC motor, a hydraulic oil pump, and a hydraulic motor,

providing power for drive and tunneling systems. The driving system comprises two groups of driving drums. The drums are linearly distributed, each equipped with an independent hydraulic motor to ensure the drum's independent operation. The excavation system includes a vertical shaft, a cross shaft, and four sets of drums. The vertical shaft is rigidly connected to the cross shaft. Each shaft of the cross shaft is connected to three sets of drums, and eight picks are equidistantly installed on the drum. A hydraulic motor is installed at the upper end of the vertical shaft to provide power for the excavation system. During the construction, the pick invades the rock mass under the action of the gravity of the body, and then the hydraulic motor drives the excavation system to rotate through the vertical axis. At this time, the pick completes rock breaking under the combined action of drum rotation inertia and shear force. When a rock is broken, the new shaft boring machine travels to the next rock breaking site according to the preset route under the control of the drive system. A layer of rock has been completely broken when the roadheader follows the set route. After cleaning the gravel, the new shaft boring machine continues to break the rock according to the preset route, so as to cycle until the shaft is excavated to the target depth.



(**a**) Boring machine side diagram



(**b**) Boring machine rear view

Figure 1. Schematic diagram of the structure of the body of the new shaft-digging machine.

In the construction process, it is necessary to obtain the positioning information, such as the position, moving speed, and attitude of the new shaft boring machine. It is difficult for a single positioning system to meet the engineering requirements, and the underground environment is relatively closed. The satellite positioning system cannot operate normally. Considered comprehensively, it was decided to use multi-sensor fusion positioning technology to realize the comprehensive positioning of the new shaft boring machine. Multi-sensor fusion positioning is a very complex and profound technology. We will conduct in-depth research in another paper, which is not described in detail here. In simple terms, we combine the ultra-wideband positioning system and the inertial navigation positioning system

to make them complementary, and we can obtain comprehensive positioning information while overcoming the engineering environment.

2.2. The Trajectory of the New Shaft Boring Machine

The structure and the rock-breaking principle of the new shaft boring machine differ from those of the ordinary boring machine. Therefore, a special driving trajectory is designed, as shown in Figure 2. The gray curve represents the shaft contour, which is the excavation range and the movable range of the boring machine. The black line is the contour of the boring machine, indicating the position of the boring machine; the blue line indicates the area excavated by the boring machine after a single excavation; the adjustment of the two excavation intervals can completely cover the shaft range; the purple line and the red line represent the driving routes of the right and left drive wheels during the boring machine's movement, respectively; and the brown line represents the movement route of the tunneling system when driving the boring machine. It can be seen that the tunneling system is kept within the movable range during the entire tunneling process. The yellow line indicates the driving route of the boring machine, and the center of the boring machine driving system follows the line during a single excavation. The green line is the transition route of the boring machine, which can be used to adjust the position of the boring machine in the two excavation processes.

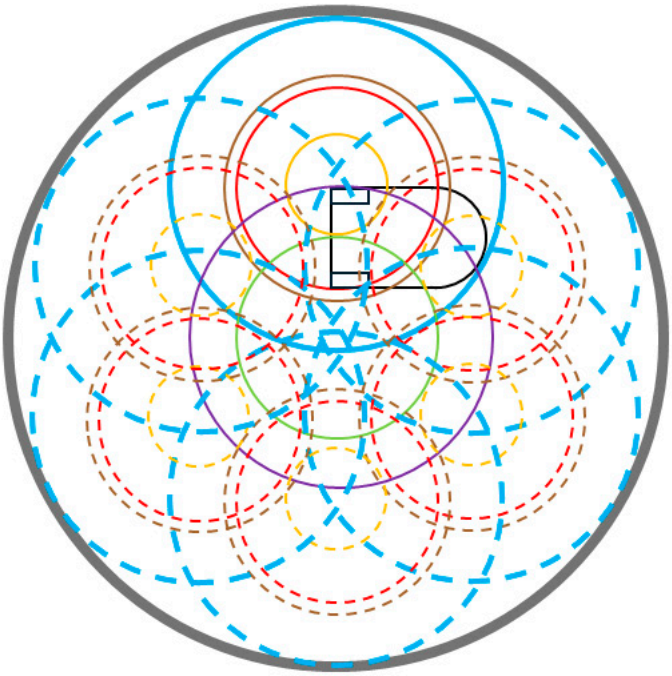


Figure 2. Travelling trajectory of the new shaft digger.

The trajectory of the new shaft boring machine has been carefully designed and completed before the implementation of this study, which is already an established known condition. All of the relevant data required for the follow-up are obtained through a series of operations, such as the analysis and derivation of the preset trajectory coordinates. In this way, based on these data obtained from the trajectory coordinates, the operation status of the new shaft boring machine can be better controlled and adjusted to ensure that it can carry out the excavation work stably and efficiently according to the established trajectory.

In the actual field construction, the shaft excavation operation has its own characteristics and process requirements. The shaft cannot successfully reach the predetermined target

depth through only one excavation. It is often necessary to clean up the gravel generated during the excavation process, and then repeat the excavation work.

Therefore, when the circular excavation is carried out for the second time, even if there is a repeated excavation of the part that has been excavated for the first time, from the perspective of the actual operation of the construction and the rationality of the overall process, this is completely acceptable and not a problem. This is a normal phenomenon that conforms to the law of shaft excavation construction and will not cause substantial adverse effects on the entire construction process.

Due to the fuselage's special structure and driving trajectory, a control scheme must be designed for the special trajectory to achieve the downhole trajectory tracking.

2.3. Control Mechanism and Process

The trajectory tracking control mechanism is shown in Figure 3, which mainly comprises driving wheel speed control and boring machine running trajectory tracking control modules. The algorithms used include the PID control algorithm and pure tracking control algorithm. The PID algorithm is responsible for controlling the moving speed of the boring machine. In contrast, the pure tracking control algorithm controls the boring machine to travel according to the preset route.

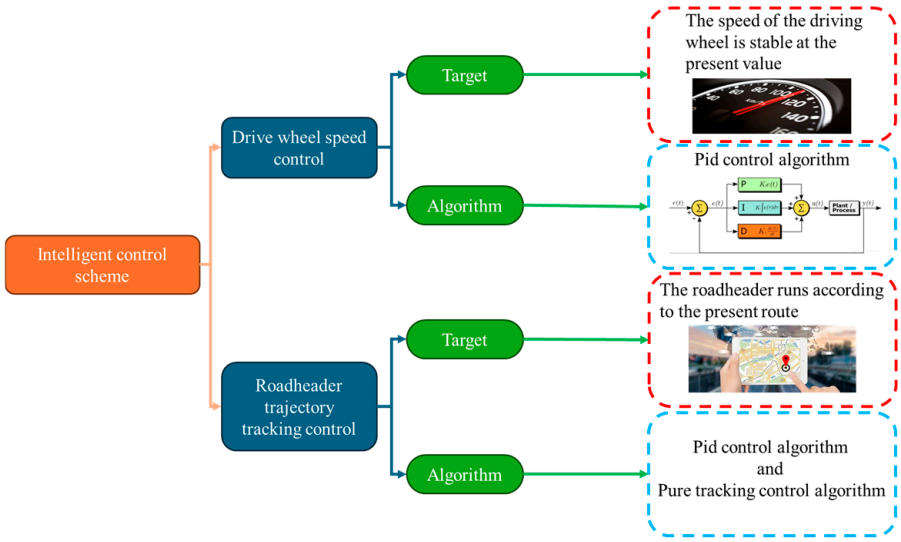


Figure 3. Trajectory tracking control mechanism.

The control process of the new shaft boring machine is shown in Figure 4:

(1) The driving trajectory of the boring machine is preset and discretized;
(2) The total station and other measurement data are used to calibrate the initial position of the boring machine;
(3) The forward distance and angle are set;
(4) The distance and angle between the boring machine and the discrete point are calculated;
(5) Prospective points meeting the requirements are screened;
(6) The control command is issued according to the relationship between the angle and the size of the angle;
(7) The boring machine position is calculated using the two-wheel differential car model;
(8) Steps 4–7 are repeated until the boring machine reaches the endpoint.

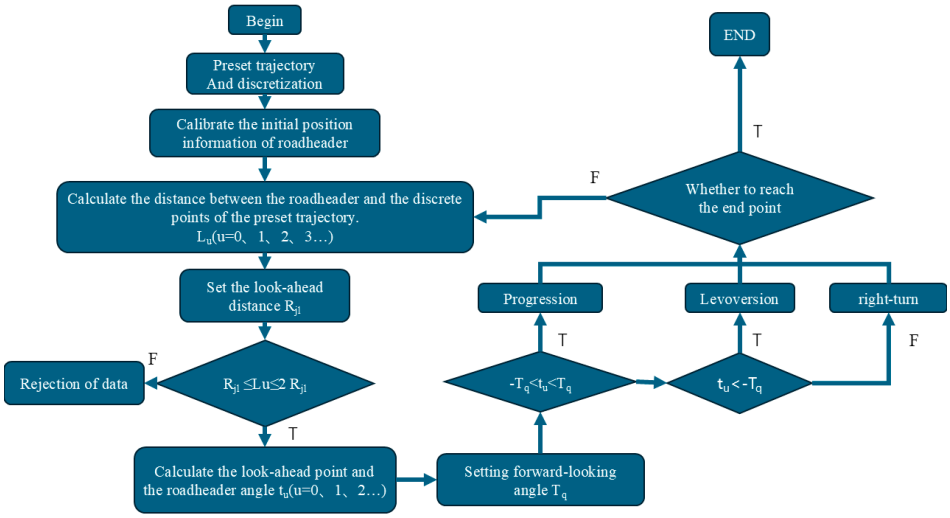


Figure 4. Driving control process.

2.4. Control System

After determining the trajectory tracking control mechanism, the control system can be designed. It can be known from the control mechanism and control process that the preset trajectory needs to be discretized first, and then the direction error and position error of the car position and each discrete point of the trajectory are calculated. Finally, the controller and the boring machine motion model are used to control the car to travel according to the preset trajectory. Because the whole process involves multiple steps such as trajectory discretization, numerical calculation, and control system design, a reliable numerical simulation software is needed.

MATLAB R2022a is a commercial mathematical software produced by MathWorks in the United States. It is used in data analysis, wireless communication, deep learning, image processing and computer vision, signal processing, quantitative finance and risk management, robots, control systems, and other fields. Simulink is a visual simulation tool in MATLAB R2022a. Simulink is a modular diagram environment for multi-domain simulation and model-based design. It supports system design, simulation, automatic code generation, and continuous testing and verification of embedded systems. Simulink provides a graphical editor, a customizable module library, and a solver for dynamic system modeling and simulation. Based on the reliability of MATLAB software and a wide range of applications, this paper chooses to use MATLAB software for numerical simulation.

2.4.1. Trajectory

From Figure 2, it can be seen that the trajectory of the boring machine is mainly composed of circles, including one large circle and six small circles. As the transition route of the boring machine, the large circle trajectory needs to be divided into six parts on average, which is responsible for connecting each small circle to each other. According to the above content, the trajectory can be expressed by the following function:

No. 1 small circle trajectory:

$$x_1^2 + (y_1 - 3)^2 = 1 \tag{1}$$

No. 2 small circle trajectory:

$$(x_2 - 1.5\sqrt{3})^2 + (y_2 - 1.5)^2 = 1 \tag{2}$$

No. 3 small circle trajectory:

$$(x_3 - 1.5\sqrt{3})^2 + (y_3 + 1.5)^2 = 1 \tag{3}$$

No. 4 small circle trajectory:

$$x_4{}^2 + (y + 3)^2 = 1 \tag{4}$$

No. 5 small circle trajectory:

$$(x_5 + 1.5\sqrt{3})^2 + (y_5 + 1.5)^2 = 1 \tag{5}$$

No. 6 small circle trajectory:

$$(x_6 + 1.5\sqrt{3})^2 + (y_6 - 1.5)^2 = 1 \tag{6}$$

Big circle trajectory:

$$x_7{}^2 + y_7{}^2 = 4 \tag{7}$$

where $(x_i, y_i)(i = 1, 2, 3, \ldots 7)$ is the center coordinates of each circular trajectory, m.

Use MATLAB software to draw the above function curves. Because MATLAB can only draw according to the planned data points in turn when drawing, it is necessary to summarize the various function curves together. The transition route is divided into six parts on average from the point to the counterclockwise direction. Each part is interspersed between two small circular trajectories, which is responsible for connecting each small circular trajectory together.

2.4.2. Trajectory Deviation Calculation

After the discrete trajectory is obtained, the position deviation between the boring machine and the discrete points on the trajectory can be calculated. As is shown in Figure 5, the main calculation items are the angle error and distance error from the boring machine to the trajectory discrete point. The calculation of distance error is very easy, which is not described here. The angle error is mainly solved by the formula.

$$\theta = \text{atan2}((x_d - x_m)/(y_d - y_m)) \tag{8}$$

θ is the expected angle, °;
(x_d, y_d) is the expected position of the boring machine, m;
(x_m, y_m) is the current position of the boring machine, m.

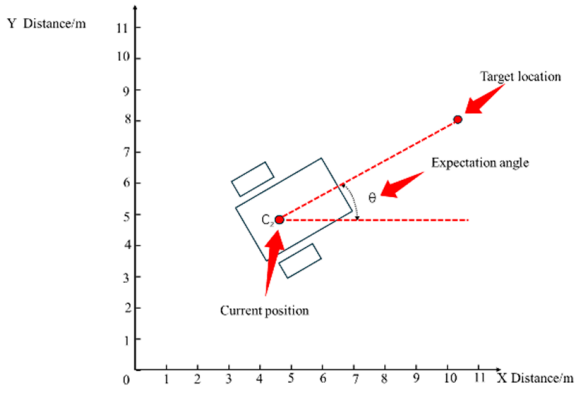


Figure 5. Position orientation of the boring machine.

2.4.3. Trajectory Deviation Adjustment

The PID algorithm is a feedback control strategy widely used in industrial control systems. It adjusts the output of the control system through the combination of proportional, integral, and differential links and finally adjusts the expected value to the target value. The core of the PID algorithm is based on the accumulation of past errors, the size of current errors, and the prediction of future errors. Then, the control output is calculated. The control principle is shown in Figure 6.

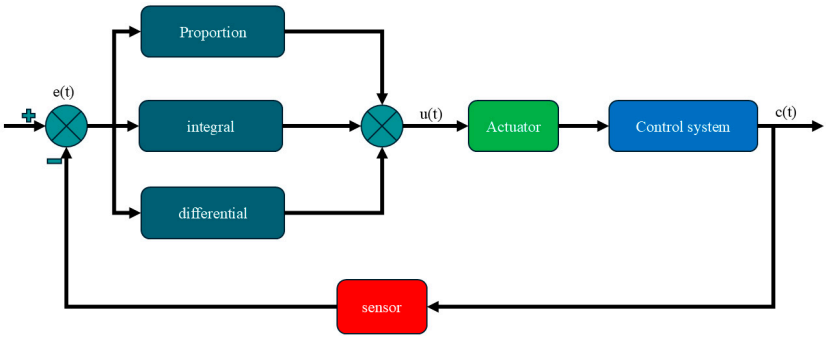


Figure 6. PID control principle diagram.

The differential equation of the PID controller corresponding to the control principle is:

$$u(t) = K_p e(t) + K_i \int_0^t e(t)dt + K_d \frac{de(t)}{dt} \tag{9}$$

$e(t)$ is the error between the expected value and the output signal;
$u(t)$ is the control signal;
K_P is the proportional constant;
K_i is the integral constant;
K_d is the differential constant.

The PID algorithm can be used to control the linear velocity and angular velocity of the boring machine so that the current angle of the boring machine is close to the expected angle and so then the current position of the boring machine is close to the expected position.

2.4.4. Controller

Through the structure of the new shaft boring machine, it can be known that the control system cannot directly control the linear velocity and angular velocity of the boring machine. The control system can only control the linear speed and angular velocity of the boring machine by adjusting the speed of the left driving wheel and the right driving wheel of the boring machine. Therefore, before designing the controller, the relationship between the speed of the left drive wheel and the speed of the right drive wheel of the boring machine and the linear speed and angular speed of the boring machine must be obtained. According to the rigid body mechanics, the relationship between the speed of the two driving wheels of the boring machine and the linear speed and angular speed can be obtained as follows:

$$\begin{bmatrix} v_r \\ v_l \end{bmatrix} = \begin{bmatrix} 1/2 & 1/2 \\ 1/H & -1/H \end{bmatrix}^{-1} \begin{bmatrix} v \\ \omega \end{bmatrix} \tag{10}$$

where ω represents the angular velocity of the boring machine, $r/\min$; v_1 and v_2 represent the left wheel speed and the right wheel speed of the boring machine, $m/\min$; H repre-

sents the wheel spacing, m; and v represents the speed of the center point of the boring machine, m/min.

2.4.5. Motion Model

According to the structure of the new shaft boring machine, the body is provided with forward power and steering torque by two driving wheels. Therefore, the boring machine can be simplified into a two-wheel differential car model, and kinematics modeling can be carried out. As shown in Figure 7, the motion mode of the two-wheel differential balance trolley is roughly divided into linear and circular motion. When it is equal to the size and is in the same direction, the boring machine makes a linear motion; when the boring machine is not equal to the size and in the same direction, it moves around the center of the circle O; and when the boring machine is equal in size and opposite in direction, the boring machine rotates around its center [19–21]. The shaft boring machine is mainly circular motion, and its motion radius, angular velocity, and linear velocity are as follows:

$$R_b = H \times (v_r + v_l)/2(v_r - v_l) \tag{11}$$

$$\begin{pmatrix} v \\ \omega \end{pmatrix} = \begin{pmatrix} 1/2 & 1/2 \\ 1/H & -1/H \end{pmatrix} \begin{pmatrix} v_r \\ v_l \end{pmatrix} \tag{12}$$

$$\begin{pmatrix} \dot{x}_c \\ \dot{y}_c \\ \dot{\theta} \end{pmatrix} = \begin{pmatrix} \cos\theta & 0 \\ \sin\theta & 0 \\ 0 & 1 \end{pmatrix} \begin{pmatrix} v \\ \omega \end{pmatrix} \tag{13}$$

where R_b represents the distance from the boring machine to the center of the circle, m; x_c and y_c are the coordinates of the boring machine, m; $\dot{x}_c$ and $\dot{y}_c$ represent the moving speed of the new shaft boring machine in the X- and Y-axis directions, m/s; and θ is the heading angle of the boring machine.

2.4.6. Transfer Function

The new shaft boring machine can be regarded as a two-wheel differential car according to its movement structure. The motion control of two-wheel differential car is divided into distance control and direction control. The transfer function is modeled for these two parts.

The input torque of the two-wheel differential car is T, and the output is the steering angle of the car θ. According to the application of Newton's second law in rotational motion, for a system with moment of inertia b and damping coefficient b, the kinetic equation is

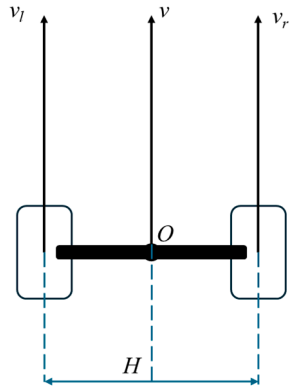
$$J\frac{d\theta}{dt} + b\theta = T \tag{14}$$

Applying the Laplace transform to the above formula yields:

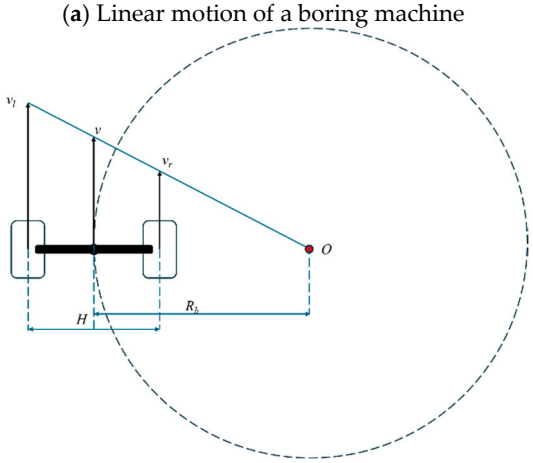
$$(Js + b)\theta(s) = T(s) \tag{15}$$

Then, the direction control transfer function is:

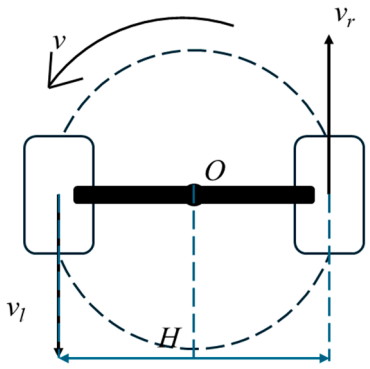
$$G(s)_1 = \frac{\theta(s)}{T(s)} = \frac{1}{Js + b} \tag{16}$$



(**a**) Linear motion of a boring machine



(**b**) Circular motion of a boring machine



(**c**) In situ circular motion of a boring machine

Figure 7. Circular motion trajectory of a boring machine.

The distance control transfer function is introduced below, assuming that when the two-wheel differential trolley moves in a straight line, it is subjected to a driving force F, the mass of the trolley is m, the damping force $F_d = -bv$ is proportional to the velocity, and there is elastic force kv exerted by the environment, where k is the equivalent elastic coefficient, according to Newton's second law:

$$F - F_d - kv = m\frac{dv}{dt} \tag{17}$$

And because $v = \frac{dx}{dt}$, where x represents the position of the car, that is, the distance variable, the following can be obtained:

$$m\frac{dx^2}{dt^2} + bv + kv = F \tag{18}$$

Applying the Laplace transform to the above formula, we obtain:

$$(ms^2 + bs + k)X(s) = F(s) \tag{19}$$

Then, the transfer function can be expressed as:

$$G(s)_2 = \frac{X(s)}{F(s)} = \frac{1}{ms^2 + bs + k} \tag{20}$$

We plug the parameters into the formula to obtain:

$$G(s)_1 = \frac{1}{20833.33s - 5000} \tag{21}$$

$$G(s)_2 = \frac{1}{10000s^2 - 5000s + 5} \tag{22}$$

2.5. Numerical Simulation System Construction

The general idea of the trajectory tracking control principle of the new shaft boring machine is as follows:

(1) Calculate the coordinate relationship between the boring machine and the target point;
(2) The control command is issued according to the coordinate relationship to control the boring machine to move to the specified target point;
(3) Update the target point coordinates and repeat the above steps until the boring machine travels according to the set trajectory.

The control system model is built based on the above ideas using MATLAB and Simulink software. First, in MATLAB, the trajectory of the new shaft boring machine designed in Section 2.2 is discretized to obtain the target coordinate point. Then, it is transmitted to Simulink. Next, the expected angle and position error are calculated according to the relationship between the current position and the target position in Simulink. Then, the PID controller is used to adjust the angular velocity and linear velocity of the boring machine based on the angle error and angle error. Hence, the boring machine can reach the specified target point. Finally, the target point coordinates are updated, and the appeal step is repeated until the boring machine is completed according to the set route.

The specific Simulink model and the functions of each module are shown in Figure 8.

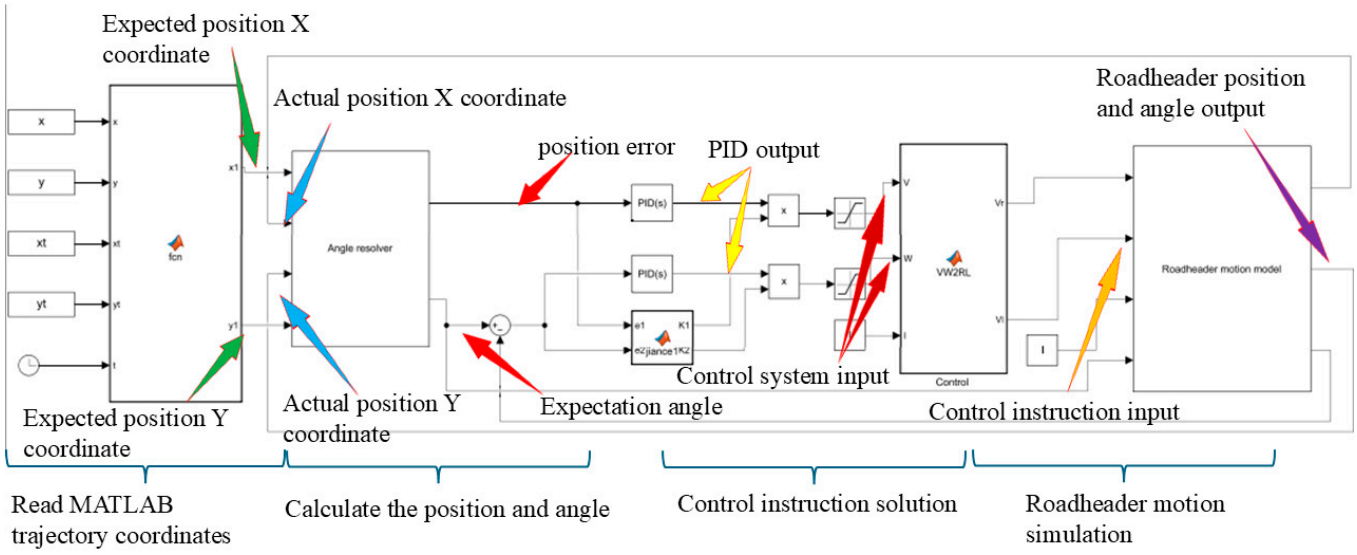


Figure 8. Simulink simulation model of new shaft boring machine.

3. Results and Discussion

The results given in this paper include numerical simulation and field tests. The numerical simulation was carried out by using MATLAB and Simulink. MATLAB was responsible for designing the underground moving path of the boring machine. Simulink was responsible for designing the control system and the boring machine motion model. Finally, MATLAB was used to draw the numerical simulation results. In order to verify the reliability of the numerical simulation results, we conducted field tests on the cement ground near the mine. Using the data obtained from the numerical simulation to control the driving system of the new shaft boring machine, the tracking operation process of the boring machine and the ground crushing results were recorded, which prove the reliability of the numerical simulation.

3.1. Boring Machine Trajectory Tracking Model Establishment and Parameter Definition

The control system model is built in Simulink, and the motion model of the two-wheel differential car in Section 2.4.5 is used as the mathematical basis. The motion model of the boring machine is shown in Figure 9. By inputting the speed of the two driving wheels, the distance between the driving wheels and the heading angle of the car at the previous moment and the position coordinates and heading angle of the car at the next moment are calculated.

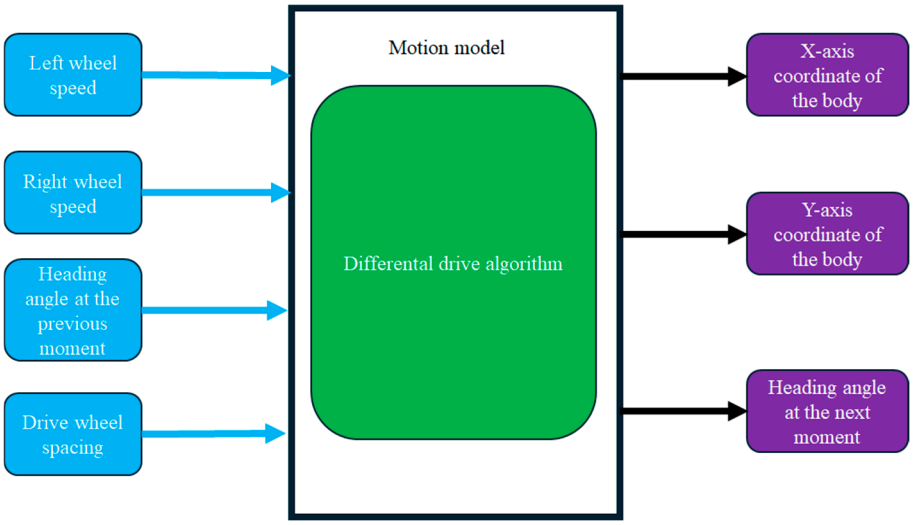


Figure 9. Simulink movement model of boring machine.

The northeast coordinate system was established with the center of the shaft as the origin of the coordinate, the east direction as the X-axis, and the north direction as the Y-axis. According to the structure size, model operation formula, and trajectory coordinate of the new shaft boring machine, the simulation test parameters are set as shown in Table 1, Table 2, and Table 3, respectively. The boring machine is 3 m long, 2 m wide, and weighs 10 t. The trajectory tracking of the new shaft boring machine can be divided into two parts: direction control and distance control. The direction control can be regarded as a first-order system, so the Ziegler–Nichols method was selected to calculate the matching PID parameters. The distance control can be regarded as a second-order system, and the particle swarm optimization algorithm can be used to tune the PID parameters. In another article by the authors [22], the authors conducted in-depth research on this, which is not repeated here. The parameters of the linear velocity PID controller are set to $K_p = 9.3$, $K_i = 1.8$, and $K_d = 1.0$, while the parameters of the angular velocity PID controller are set to $K_p = 1.8$, $K_i = 1.8$, and $K_d = 0.45$. The trajectory coordinate settings are as follows: the shaft radius

is 6 m, the radius of the excavation route is 3.3 m, and the radius of the transition route is 2.76 m. The first excavation route coordinates are $x_1 = 0$ and $y_1 = 3$, the second excavation route coordinates are $x_2 = 2.598$ and $y_2 = 1.5$, the third excavation route coordinates are $x_3 = 2.598$ and $y_3 = -1.5$, the fourth excavation route coordinates are $x_4 = 0$ and $y_4 = -3$, the fifth excavation route coordinates are $x_5 = -2.598$ and $y = -1.5$, and the sixth excavation route coordinates are $x_6 = -2.598$ and $y_6 = 1.5$.

Table 1. Body size parameters of the boring machine.

Boring Machine Length (m)	Boring Machine Width (m)	Boring Machine Weight (t)
3	2	10

Table 2. Control system parameters.

	K_d	K_i	K_d
Linear speed controller parameters	9.3	1.8	1.0
Angular velocity controller parameters	1.8	1.8	0.45

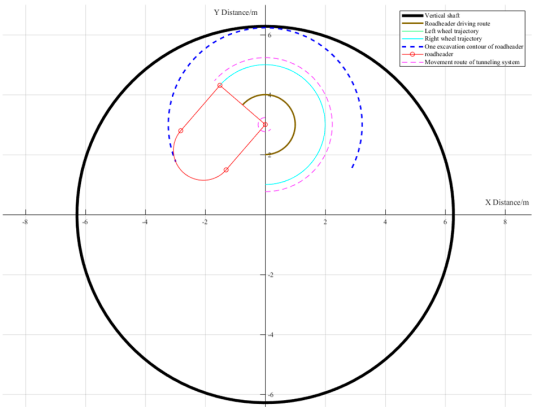
Table 3. Trajectory parameters.

	Center X Coordinate (m)	Center Y Coordinate (m)	Radius (m)
Vertical shaft	0	0	6
The first excavation route	0	3	3.3
Second excavation route	2.598	1.5	3.3
The third excavation route	2.598	−1.5	3.3
The fourth excavation route	0	−3	3.3
The fifth excavation route	−2.598	−1.5	3.3
The sixth excavation route	−2.598	1.5	3.3
Transition route	0	0	2

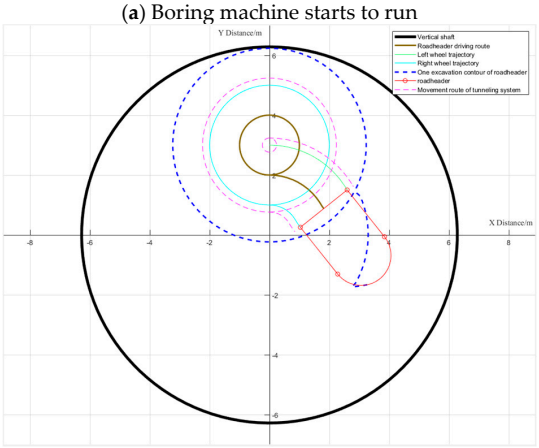
3.2. Numerical Simulation of Trajectory Tracking

The trajectory tracking process of the new shaft boring machine can be regarded as the process of two-wheel differential car driving according to the established trajectory. The boring machine's trajectory tracking effect is solved in the joint simulation environment of MATLAB and Simulink.

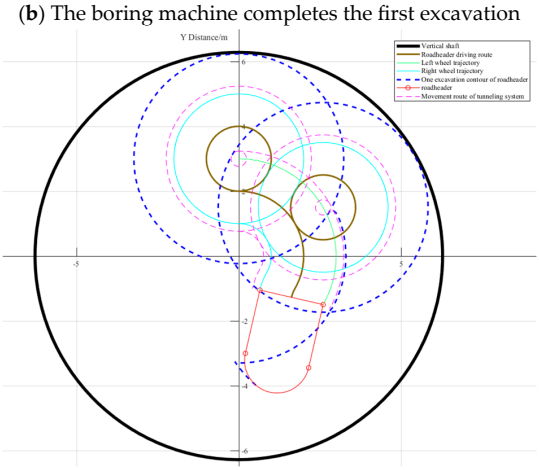
The speed of the right driving wheel is greater than that of the left driving wheel in the initial stage of the new shaft boring machine. Therefore, the body runs in a counterclockwise direction. According to Figure 10a, when the boring machine is running, the body and the tunneling system are driven according to the preset route and always remain within the shaft range. Because the driving route of the tunneling system is tangential to the edge of the shaft, the shaft excavation does not leave a corner.



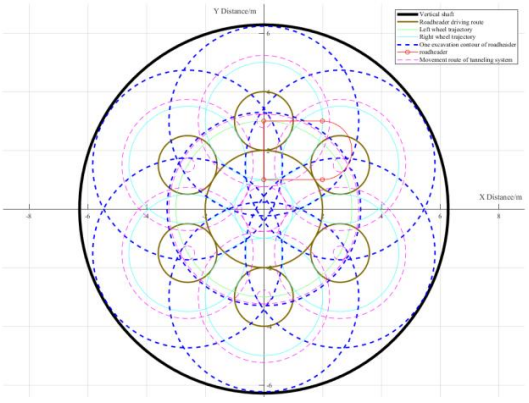
(**a**) Boring machine starts to run



(**b**) The boring machine completes the first excavation



(**c**) The boring machine enters the second excavation path through the over route



(**d**) Boring machine completes the excavation

Figure 10. Track tracking process of TBM.

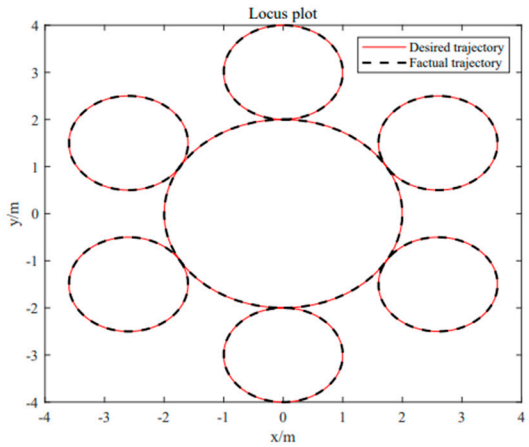
When the new shaft boring machine completes the first excavation according to the route, the ground within a radius of 3.3 m is completely covered by the boring machine, as shown in Figure 10b. Hence, it is shown that the boring machine can ensure that the ground within a radius of 3.3 m is fully excavated according to the route.

Once the new shaft boring machine completes the first excavation, the speed of the left driving wheel is adjusted to be greater than the speed of the right driving wheel. Therefore, the body moves clockwise through the overroute into the second excavation path and starts the second excavation. Figure 10c shows that the designed transition route can connect the two excavation paths. Consequently, the boring machine can complete continuous excavation.

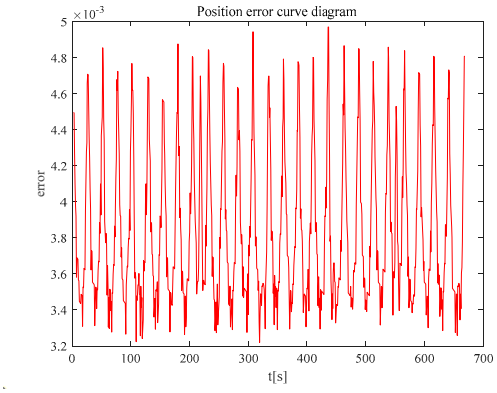
The above steps are executed cyclically according to Figure 10d. Finally, the boring machine can run smoothly along the set route within the shaft range and complete the excavation task. In the later stage, all areas within the shaft range can be excavated by adjusting the number of excavations and reducing the spacing between the two excavations.

3.3. Trajectory Tracking Data Analysis

The trajectory tracking simulation is carried out for the design route and the motion model of the new shaft boring machine. The simulation results are shown in Figure 11. According to Figure 11a,b, the actual trajectory of the boring machine completely coincides with the expected trajectory under the control system designed in this paper. The error is always kept in the range of 0.0032 m∼0.005 m, and the tracking effect is good.



(**a**) Boring machine moving trajectory

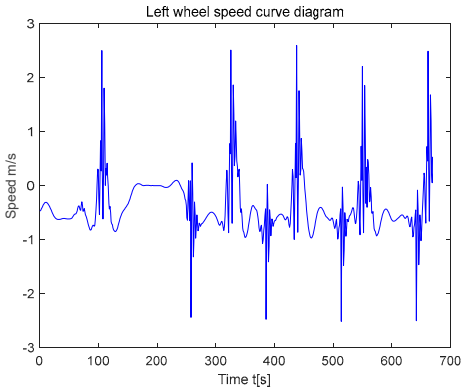


(**b**) Position tracking error

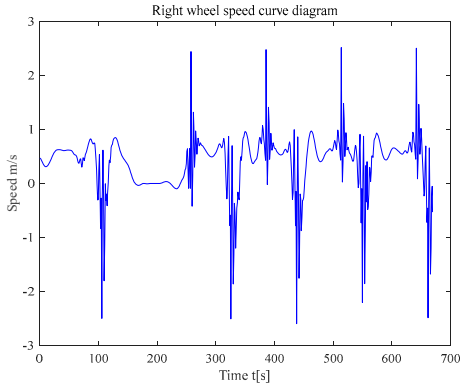
Figure 11. Simulation results of the trajectory tracking.

The speed curve of the driving wheel of the new shaft boring machine during trajectory tracking simulation is shown in Figure 12. According to Figure 12a,b, the speed change

trend of the left and right driving wheels is always opposite with significant periodicity. According to the analysis of the motion model and trajectory characteristics of the boring machine, the boring machine uses the speed difference of the driving wheel to achieve. Moreover, the steering driving and the design trajectory are characterized by repeatability, leading to the periodicity and repeatability of the speed curve.



(**a**) Left wheel speed curve



(**b**) Right wheel speed curve diagram

Figure 12. Speed curve of the driving wheel of new shaft boring machine.

The above is the result of the numerical simulation of the trajectory tracking of the new shaft boring machine using the PID algorithm. In addition to the PID algorithm, the LQR algorithm or MPC algorithm can also be used, but some defects of these algorithms need to be paid attention to. As an optimal algorithm, the LQR algorithm has a strong dependence on the system model. Even if there is a small modeling deviation, the control performance will be greatly reduced. Especially in the control of machinery with strong vibration, the control performance of the LQR algorithm is often not as good as that of the PID algorithm [23]. The new shaft boring machine will inevitably have a strong vibration in the process of rock breaking, so the LQR algorithm is not suitable for controlling the rock-breaking machine. In addition to being extremely dependent on the system model, the MPC algorithm also has defects such as high computational complexity, difficulty in parameter adjustment, poor real-time performance, and high communication requirements. Shaft excavation attaches great importance to the real-time operation of machinery, and the existence of a large number of mechanical equipment in the underground environment does not guarantee smooth communication, so MPC is not suitable for the control of shaft excavation machinery. Compared with the LQR and MPC algorithms, the PID algorithm has significant advantages. Its principle is simple and easy to operate, and it has low dependence on the system model, high control accuracy, and strong anti-interference ability. In recent years, it has shown very good improvement potential [24], which is very suitable for the control of new shaft boring machines.

3.4. Trajectory Tracking Field Experiments

The field trajectory tracking test is carried out near the mine to test the actual operation effect of the trajectory tracking scheme, as shown in Figure 13. The speed data of the left and right driving drum of the boring machine in the MATLAB trajectory tracking simulation test in the previous chapter were input to the console, and the speed of the left and right driving wheel of the boring machine was controlled by the console. Then, the actual operation trajectory of the boring machine was observed, and the test results are compared with the simulation ones.



Figure 13. Field experiment of the new shaft boring machine.

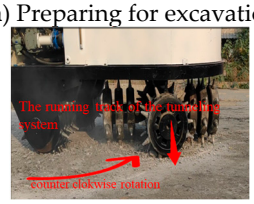
The trajectory tracking process of the new shaft boring machine can be regarded as a two-wheel differential car driving according to the set trajectory. Due to the limited space and the great repeatability of the set trajectory, only the running part of the boring machine is controlled to compare the running results with the set trajectory. The field test of the new shaft boring machine is shown in Figure 14.



(**a**) Preparing for excavation



(**b**) Start mining



(**c**) Excavation system movement



(**d**) Rock breaking



(**e**) Traveling according to the trajectory



(**f**) Go to the next digging point

Figure 14. Field test process of the new shaft boring machine.

When the new boring machine starts to excavate, the pick invades the cement ground by relying on the self-weight of the body. Then, the hydraulic motor drives the roller to rotate through the vertical and cross axes. The cement ground, in contact with the tunneling system, starts to be damaged, as shown in Figure 14b. In the early stage of

damage, the accumulation of cement fragments at the bottom of the body is relatively low, and the ground is hard. Hence, the body vibrates, but the position of the body is minorly affected. As the ground is gradually destroyed, large blocks of cement are stripped from the ground and gradually accumulated at the bottom of the body. This body plays a buffer role, gradually slowing the body's vibration. Finally, the excavation system crushes large pieces of cement to form a circular excavation surface, as shown in Figure 15. Compared with the simulation experiment, position errors can be found in the entire process of boring machine operation, indicating that the external factors such as the broken surface will cause a slight change in the position of the body.

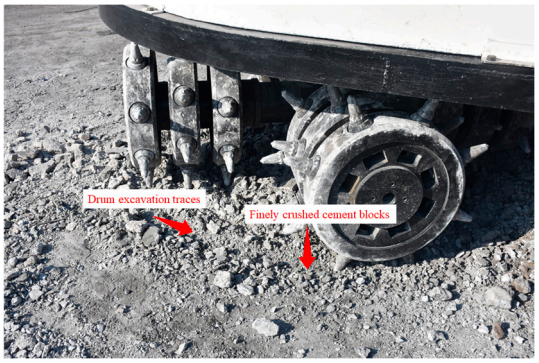


Figure 15. Circular excavation face.

When the ground contact with the tunneling system is broken, the driving system of the new shaft boring machine starts to drive the body and move according to the preset trajectory. The cement in the contact area of the driving system is peeled off, as shown in Figure 14c. The body's movement makes the driving system move along the preset trajectory. The unexcavated area in the center of the map is also fragmented. When the boring machine travels counterclockwise according to the trajectory for one week (Figure 14d), the cement is destroyed within the radius of 3.3 m, with the left driving wheel of the boring machine serving as the center radius. This result is in line with the results of the simulation experiment.

When the ground is completely broken, the boring machine travels to the next excavation point according to the trajectory, as shown in Figure 14e,f. The cycle is repeated until the ground cement is completely broken. It can be observed that the boring machine's running track and excavation area are in line with the simulation results.

In summary, the field trajectory tracking test results and MATLAB simulation experiment of the new shaft boring machine are compared and analyzed. The trajectory tracking scheme designed in this paper can control the shaft boring machine to achieve the full-section excavation of the shaft, further validating the rationality of the simulation experiment.

4. Conclusions

In this paper, a control system based on the PID algorithm was designed for the special motion model and running track of the new shaft boring machine. The control instructions were issued by analyzing the relationship between the trajectory and the body's position. Moreover, the PID algorithm was used to control the speed of the two driving wheels and the running trajectory of the boring machine. The tracking effect of the new shaft boring machine for a specific trajectory was simulated through the joint simulation of MATLAB and Simulink. The actual running trajectory of the new shaft boring machine almost completely coincides with the expected trajectory. At the same time, the position error is less than 0.005 m. This observation shows that the control system designed in this

paper can achieve precise trajectory tracking control for the new shaft boring machine. Combined with the simulation test of underground trajectory tracking of the new shaft boring machine, the field test of trajectory tracking of the new shaft boring machine is set up. The test results show that the new shaft boring machine can carry out continuous mining according to the preset route, which is consistent with the simulation test results.

Author Contributions: Writing—review and editing, J.S.; Conceptualization, J.S. and X.C.; Supervision, H.J.; Investigation, Q.W. and D.Z.; Resources, Y.H. and Z.L. All authors have read and agreed to the published version of the manuscript.

Funding: This research was funded by National Key R&D Program (2023YFC2907203), National Natural Science Foundation General Fund Project (52374121), Henan Province Science and Technology Research and Development Joint Fund (235200810016).

Data Availability Statement: No new data were created or analyzed in this study. Data sharing is not applicable to this article.

Conflicts of Interest: The authors declare no conflict of interest.

References

1. Mao, J.; Yang, R.; Xie, M.; Lu, J.; Wang, H.; Liu, Z.; Wang, S. Research status and prospects of key technologies for intelligent rapid excavation in coal mines. *J. China Coal Soc.* **2024**, *49*, 1214–1229.
2. Wang, G.; Zhang, L.; Li, S.; Li, S.; Feng, Y.; Meng, L.; Nan, B.; Du, M.; Fu, Z.; Li, R.; et al. Progresses in theory and technological development of unmanned smart mining system. *J. China Coal Soc.* **2023**, *48*, 34–53.
3. Yang, J.; Gao, Q. Study on construction experience of intelligent tunneling system in coal mine. *Coal Sci. Technol.* **2022**, *50*, 303–309.
4. Wang, G. New technological progress of coal mine intelligence and its problems. *Coal Sci. Technol.* **2022**, *50*, 1–27.
5. Ma, H.; Wang, S.; Mao, Q.; Shi, Z.; Zhang, X.; Yang, Z.; Cao, X.; Xue, X.; Xia, J.; Wang, C. Key common technology of intelligent heading in coal mine roadway. *J. China Coal Soc.* **2021**, *46*, 310–320.
6. Wang, Y.N.; Jiang, Y.-M.; Jiang, J.; Zhang, H.; Tan, H.-R.; Peng, W.-X.; Wu, H.-T.; Zeng, K. Key Technologies of Robot Perception and Control and Its Intelligent Manufacturing Applications. *Acta Autom. Sin.* **2023**, *49*, 494–513.
7. Zhu, Q.; Cheng, J.; Chen, X.; Yang, C.; Gao, Y.; Shao, G. Review on Path Tracking Control of Unmanned Articulated Steering Vehicles. *J. Agric. Mach.* **2024**, *55*, 1–21.
8. He, H.; Liu, Q.; Shentu, S.; Gong, Z. Trajectory Tacking Controller Design for Wheeled Robots in Multi-robot Cooperative Transport. *J. Mech. Eng.* **2024**, *60*, 145–155.
9. Fu, T.; Zhang, T.; Cui, Y.; Song, X. Deep Learning-enhanced Intelligent Electric Shovel Digging Trajectory Tracking Control. *J. Mech. Eng.* **2024**, *60*, 357–366.
10. Zhu, G.; Cui, G.; Ma, Q.; Li, Z. Predefined-time adaptive trajectory tracking control for a quadrotor UAV. *Control Theory Appl.* **2023**, *40*, 1–10. [CrossRef]
11. Li, B.; Wang, C.; Ma, L.; Xiao, B.; Gong, W. Fixed-time trajectory tracking control of a wheeled mobile robots. *Control Decis.* **2024**, *39*, 845–852.
12. Liu, J.; Feng, G.; Zhang, J.; Yang, K. Fusion Research of Trajectory Tracking Energy-saving Control of Unmanned Hybrid Vehicles. *China Mech. Eng.* **2024**, *35*, 678–690.
13. Yang, Z.; Li, S.; Wang, Z. Trajectory Tracking Control of Distributed Driving Intelligent Vehicles Based on Adaptive Variable Parameter MPC. *J. Mech. Eng.* **2024**, *60*, 363–377.
14. Liu, Y.; Wang, H.; Zhang, J.; Fan, Q. Neural Adaptive Trajectory Tracking Control for a Magnetic Microrobot. *Robot* **2023**, *45*, 683–690.
15. Shen, Y.; Zhang, Y.; Liu, H.; He, S.; Feng, R.; Wan, Y. Research Review of Agricultural Equipment Automatic Control Technology. *Trans. Chin. Soc. Agric. Mach.* **2023**, *54*, 1–18.
16. Zhang, J. Research on Dynamic Failure of Frozen Soil Under the Rolling Cutter of New Vertical Shaft Tunnelling. Master's Thesis, Henan Polytechnic University, Jiaozuo, China, 2022.
17. Zhang, J.; Li, X.; Chen, X.; Jiao, H.; Li, Z. Numerical simulation study on the influencing factors of truncated rolling excavation process in frozen soil. *J. Glaciol. Geocryol.* **2022**, *44*, 229–240.
18. Chen, X.; Zhang, J.; Jiao, H.; Li, Z.; Du, F.; Yang, L.; Zhang, B. Rock breaking mechanism of rolling cutter of new gravity vertical shaft continuous heading machine. *J. Min. Saf. Eng.* **2022**, *39*, 576–583+597.
19. Wang, M. Research on Key Technologies of Intelligent Mowers Roadbed Planning System. Master's Thesis, Hangzhou Dianzi University, Hangzhou, China, 2023; pp. 15–32.

20. Zhao, Y. Research on Drive Control of Intelligent Mower. Master's Thesis, Zhejiang University, Hangzhou, China, 2020; pp. 17–28.
21. Nian, J. Indoor Map Construction and Navigation of Mo bile Robot Based on Mutisensor Fusion. Master's Thesis, Beijing University of Posts and Telecommunications, Beijing, China, 2021; pp. 21–38.
22. Chen, X.; Sun, J. Revising the Motion Control Parameter Optimization Research of a Two-Wheel Differential Car. *Actuators* **2024**, *13*, 504. [CrossRef]
23. Ezzraimi, M.; Tiberkak, R.; Melbous, A.; Rechak, S. LQR and PID algorithms for vibration control of piezoelectric composite plates. *Mechanics* **2018**, *24*, 734–740. [CrossRef]
24. Chen, S.; Liu, J.; Wang, P.; Xu, C.; Cai, S.; Chu, J. Accelerated optimization in deep learning with a proportional-integral-derivative controller. *Nat. Commun.* **2024**, *15*, 10263. [CrossRef] [PubMed]

Disclaimer/Publisher's Note: The statements, opinions and data contained in all publications are solely those of the individual author(s) and contributor(s) and not of MDPI and/or the editor(s). MDPI and/or the editor(s) disclaim responsibility for any injury to people or property resulting from any ideas, methods, instructions or products referred to in the content.